Nanofiber-mediated radiative transfer between two distant atoms

Fam Le Kien,[1,*] S. Dutta Gupta,[1,2] K. P. Nayak,[1] and K. Hakuta[1]
[1]*Department of Applied Physics and Chemistry, University of Electro-Communications, Chofu, Tokyo 182-8585, Japan*
[2]*School of Physics, University of Hyderabad, Hyderabad, India*
(Received 26 August 2005; published 23 December 2005)

We study spontaneous emission from a pair of two-level atoms near a nanofiber. We demonstrate a substantial radiative exchange between distant atoms mediated by the guided modes of the nanofiber. The exchange is shown to lead to increased and decreased lifetimes of the subradiant and superradiant states, respectively. Our analysis is based on the full quantization of both the radiation and guided modes of the fiber in the framework of the Heisenberg-Langevin theory and the master equation formalism.

DOI: 10.1103/PhysRevA.72.063815 PACS number(s): 42.50.Ct, 42.50.Gy

I. INTRODUCTION

Controlled radiative transfer between two atoms (or molecules) has been in the focus of scientific research for the past several decades. Initial research in this area was aimed at enhancing (in terms of both range and strength) the energy transfer by means of "dressing" the environment of the donor-acceptor pair. A typical nonradiative Förster energy transfer range of $\leqslant 10$ nm was surpassed by suitable use of localized plasmons or whispering gallery modes [1–3]. Enhancement of energy transfer by two orders of magnitude was reported as early as in the mid-1980s [2]. Similar enhancements have been reported in microcavities [4,5]. Now the literature on microcavity-assisted dipole-dipole interaction is truly vast [6–9]. Very fast (approaching picosecond time scales) energy transfer was recorded in systems with quantum dots [10]. In a recent experiment it was shown that surface-plasmon-enhanced communication can be established between donor-acceptor pairs across 120-nm-thick metal films [11]. The recent directions of research on dipole-dipole interaction go much beyond the scope of the initial interest of chemical physicists. They now encompass emerging areas of few-atom spectroscopy [12], near-field optics [13], and subwavelength-resolution nano-optics [14]. Spectroscopy of two molecules separated by about 10 nm has been carried out and the resonances induced by two-photon excitation of the two molecules were reported [12]. The remarkable possibility of manipulating the degree of entanglement among them was demonstrated. The role of microspheres in controlling the entanglement has also been investigated [15]. A detailed study on the dipole-dipole interaction modified by a nanosphere has been carried out [16]. A very interesting application was a form of "telegraphy" on a dielectric microplanet, a resonant molecular "telegraphy" in relation to the donor and acceptor molecules occupying the north and south poles of a dielectric microsphere [3]. It is clear that the range of such "telegraphy" can be increased arbitrarily if one switches from microspheres to nanofibers.

In this paper, we study resonant coupling between *distant* atoms mediated by a subwavelength-diameter fiber. In a recent study we had demonstrated that about 30% of the fluorescence from a single cesium atom can be picked up by a subwavelength-diameter fiber (200 nm in radius) [17]. The suitability and advantages of subwavelength-diameter fibers for cavity QED applications [17–20] and for microscopic atom trapping [21] were discussed in detail. Our study on a two-atom system in presence of a nanofiber is general in the sense that it incorporates fully quantized contributions from guided and radiation modes for arbitrary mutual orientations and placements of the atoms. We focus our attention on the cross-decay rate and show that for large distances the effect of the radiation modes decays while substantial exchange between the atoms survives due to the guided modes. As a signature of this exchange we look at the decay behavior for the superradiant and subradiant combinations [22,23] of one-excitation two-atom states. We show that the subradiant state, even for distant atoms, decays substantially more slowly than the superradiant state.

The paper is organized as follows. In Sec. II we describe the model. In Sec. III we derive the basic equations and the characteristics of spontaneous emission. In Sec. IV we analyze the dynamics of the system. In Sec. V we present numerical results. Our conclusions are given in Sec. VI.

II. MODEL

A. Quantization of the field around a thin fiber

We consider a fiber that has a cylindrical silica core of radius a and refractive index n_1 and an infinite vacuum clad of refractive index $n_2=1$ [see Fig. 1(a)]. The positive-frequency part $\mathbf{E}^{(+)}$ of the electric component of the field can be decomposed into the contributions from the guided and radiation modes as

$$\mathbf{E}^{(+)} = \mathbf{E}^{(+)}_{\text{guided}} + \mathbf{E}^{(+)}_{\text{rad}}. \tag{1}$$

We do not take into account the evanescent modes, which do not contribute to the spontaneous emission process [18–20]. We use the cylindrical coordinates (r,φ,z) with z as the axis of the fiber. In view of the very low losses of silica in the wavelength range of interest, we neglect material absorption.

The continuum field quantization follows the procedures presented in Ref. [24]. Regarding the guided modes, we as-

*Also at Institute of Physics and Electronics, Vietnamese Academy of Science and Technology, Hanoi, Vietnam.

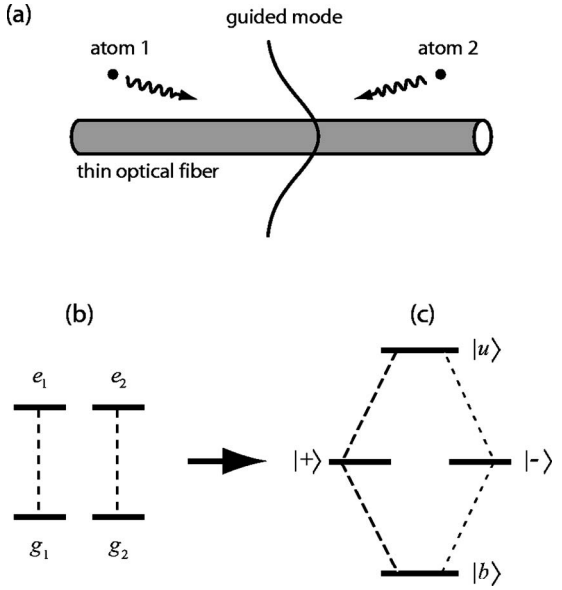

FIG. 1. (a) Two atoms in the vicinity of a thin optical fiber. (b) Scheme of levels and transitions of a pair of two-level atoms. (c) Scheme of levels and transitions in terms of superradiant and subradiant states for a pair of two-level atoms coupled to a common electromagnetic field.

sume that the single-mode condition [25] is satisfied for a finite bandwidth of the field frequency ω around the atomic frequency ω_0. We label each guided mode by an index $\mu=(\omega,f,p)$, where $f=+,-$ denotes the forward or backward propagation direction, and $p=+,-$ denotes the counterclockwise or clockwise rotation of polarization. When we quantize the field in the guided modes, we obtain the following expression for $\mathbf{E}^{(+)}_{\text{guided}}$ in the interaction picture:

$$\mathbf{E}^{(+)}_{\text{guided}} = i\sum_{fp}\int_0^\infty d\omega \sqrt{\frac{\hbar\omega\beta'}{4\pi\epsilon_0}} a_\mu \mathbf{e}^{(\mu)} e^{-i(\omega t - f\beta z - p\varphi)}. \quad (2)$$

Here β is the longitudinal propagation constant, β' is the derivative of β with respect to ω, a_μ is the respective photon annihilation operator, and $\mathbf{e}^{(\mu)}=\mathbf{e}^{(\mu)}(r,\varphi)$ is the electric-field profile function of the guided mode μ in the classical problem. The constant β is determined by the fiber eigenvalue equation (A1). The operators a_μ and $a^\dagger_\mu$ satisfy the continuous-mode bosonic commutation rules $[a_\mu, a^\dagger_{\mu'}]=\delta(\omega-\omega')\delta_{ff'}\delta_{pp'}$. The normalization of $\mathbf{e}^{(\mu)}$ is given by

$$\int_0^{2\pi} d\varphi \int_0^\infty n_{\text{rf}}^2 |\mathbf{e}^{(\mu)}|^2 r\, dr = 1. \quad (3)$$

Here $n_{\text{rf}}(r)=n_1$ for $r<a$, and $n_{\text{rf}}(r)=n_2$ for $r>a$. The explicit expression for the guided mode function $\mathbf{e}^{(\mu)}$ is given in Appendix A.

Unlike the case of guided modes, in the case of radiation modes, the longitudinal propagation constant β for each value of ω can vary continuously, from $-kn_2$ to kn_2 (with $k=\omega/c$). We label each radiation mode by the index $\nu=(\omega,\beta,m,p)$, where m is the mode order and p is the mode polarization. When we quantize the field in the radiation modes, we obtain the following expression for $\mathbf{E}^{(+)}_{\text{rad}}$ in the interaction picture:

$$\mathbf{E}^{(+)}_{\text{rad}} = i\sum_{mp}\int_0^\infty d\omega \int_{-kn_2}^{kn_2} d\beta \sqrt{\frac{\hbar\omega}{4\pi\epsilon_0}} a_\nu \mathbf{e}^{(\nu)} e^{-i(\omega t - \beta z - m\varphi)}. \quad (4)$$

Here a_ν is the respective photon annihilation operator, and $\mathbf{e}^{(\nu)}=\mathbf{e}^{(\nu)}(r,\varphi)$ is the electric-field profile function of the radiation mode ν in the classical problem. The operators a_ν and $a^\dagger_\nu$ satisfy the continuous-mode bosonic commutation rules $[a_\nu, a^\dagger_{\nu'}]=\delta(\omega-\omega')\delta(\beta-\beta')\delta_{mm'}\delta_{pp'}$. The normalization of $\mathbf{e}^{(\nu)}$ is given by

$$\int_0^{2\pi} d\varphi \int_0^\infty n_{\text{rf}}^2 [\mathbf{e}^{(\nu)}\mathbf{e}^{(\nu')*}]_{\beta=\beta',m=m',p=p'} r\, dr = \delta(\omega-\omega'). \quad (5)$$

The explicit expression for the radiation mode function $\mathbf{e}^{(\nu)}$ is given in Appendix B.

B. Interaction of a pair of two-level atoms with the quantum field

Consider two identical two-level atoms located at points (r_1,φ_1,z_1) and (r_2,φ_2,z_2), respectively [see Fig. 1(b)]. We label the atoms by the index $j=1,2$. In the interaction picture, the electric dipole of the jth atom is given by $\mathbf{D}_j=\mathbf{d}_j^*\sigma_j e^{-i\omega_0 t}+\mathbf{d}_j\sigma_j^\dagger e^{i\omega_0 t}$. Here the operators $\sigma_j=|g_j\rangle\langle e_j|$ and $\sigma_j^\dagger=|e_j\rangle\langle g_j|$ describe the downward and upward transitions, respectively, and $\mathbf{d}_j$ is the dipole matrix element. Without the loss of generality, we assume that both $\mathbf{d}_1$ and $\mathbf{d}_2$ are real.

The Hamiltonian for the atom-field interaction in the dipole approximation is given by

$$H_{\text{int}} = -i\hbar\sum_{\alpha j} G_{\alpha j}\sigma_j^\dagger a_\alpha e^{-i(\omega-\omega_0)t} - i\hbar\sum_{\alpha j} G_{\alpha j}\sigma_j a_\alpha e^{-i(\omega+\omega_0)t} + \text{H.c.} \quad (6)$$

Here we have introduced the mode index $\alpha=\mu,\nu$ and the notation $\Sigma_\alpha=\Sigma_\mu+\Sigma_\nu$, $\Sigma_\mu=\Sigma_{fp}\int_0^\infty d\omega$, and $\Sigma_\nu=\Sigma_{mp}\int_0^\infty d\omega\int_{-kn_2}^{kn_2} d\beta$. The coefficients $G_{\mu j}$ and $G_{\nu j}$ characterize the coupling of the jth atom with the guided mode $\mu=(\omega,f,p)$ and the radiation mode $\nu=(\omega,\beta,m,p)$, respectively. Their explicit expressions are

$$G_{\mu j} = \sqrt{\frac{\omega\beta'}{4\pi\epsilon_0\hbar}}[\mathbf{d}_j\cdot\mathbf{e}^{(\mu)}(r_j,\varphi_j)]e^{i(f\beta z_j+p\varphi_j)},$$

$$G_{\nu j} = \sqrt{\frac{\omega}{4\pi\epsilon_0\hbar}}[\mathbf{d}_j\cdot\mathbf{e}^{(\nu)}(r_j,\varphi_j)]e^{i(\beta z_j+m\varphi_j)}. \quad (7)$$

III. SPONTANEOUS EMISSION OF TWO ATOMS IN PRESENCE OF A THIN FIBER

Let $\mathcal{O}$ be an arbitrary atomic operator. The Heisenberg equation for this operator is

$$\dot{\mathcal{O}} = \sum_{\alpha j} (G_{\alpha j}[\sigma_j^\dagger, \mathcal{O}] a_\alpha e^{-i(\omega-\omega_0)t} + G_{\alpha j}[\sigma_j, \mathcal{O}] a_\alpha e^{-i(\omega+\omega_0)t} + G_{\alpha j}^* a_\alpha^\dagger [\mathcal{O}, \sigma_j] e^{i(\omega-\omega_0)t} + G_{\alpha j}^* a_\alpha^\dagger [\mathcal{O}, \sigma_j^\dagger] e^{i(\omega+\omega_0)t}). \quad (8)$$

Meanwhile, the Heisenberg equation for the field operators a_α is

$$\dot{a}_\alpha = \sum_j G_{\alpha j}^* \sigma_j e^{i(\omega-\omega_0)t} + \sum_j G_{\alpha j}^* \sigma_j^\dagger e^{i(\omega+\omega_0)t}. \quad (9)$$

Integrating Eq. (9), we find

$$a_\alpha(t) = a_\alpha(t_0) + \sum_j G_{\alpha j}^* \int_{t_0}^t dt' \sigma_j(t') e^{i(\omega-\omega_0)t'} + \sum_j G_{\alpha j}^* \int_{t_0}^t dt' \sigma_j^\dagger(t') e^{i(\omega+\omega_0)t'}. \quad (10)$$

We consider the situation where the field is initially in the vacuum state. We assume that the evolution time $t-t_0$ and the characteristic atomic lifetime τ_a are large as compared to the optical period $2\pi/\omega_0$ and the light propagation time $|\mathbf{r}_2-\mathbf{r}_1|/c$ between the two atoms. We consider the case where the atomic frequency is well below the cutoff frequency of the fiber. In this case, the continuum of the guided and radiation modes is regular and broadband around the atomic frequency. Under these conditions, the effect of the retardation is concealed [26], and the Markov approximation $\sigma_j(t') = \sigma_j(t)$ can be applied to describe the back action of the second and third terms in Eq. (10) on the atom. We insert the result of this approximation into Eq. (8) and neglect fast-oscillating terms. Under the condition $t-t_0 \gg 2\pi/\omega_0$, we calculate the integrals with respect to t' in the limit $t-t_0 \to \infty$. Then we obtain the Heisenberg-Langevin equation

$$\dot{\mathcal{O}} = \frac{1}{2}\sum_{ij} \gamma_{ij}([\sigma_i^\dagger, \mathcal{O}]\sigma_j + \sigma_i^\dagger[\mathcal{O}, \sigma_j]) + i\sum_{ij} \Omega_{ij}[\sigma_i^\dagger \sigma_j, \mathcal{O}] + \xi_{\mathcal{O}} \quad (11)$$

for the atomic operator $\mathcal{O}$. Here the indices i and j are equal to 1 or 2, the coefficients

$$\gamma_{ij} = \gamma_{ij}^{(\mathrm{g})} + \gamma_{ij}^{(\mathrm{r})}, \quad \Omega_{ij} = \Omega_{ij}^{(\mathrm{g})} + \Omega_{ij}^{(\mathrm{r})} \quad (12)$$

describe the decay rates and frequency shifts, and $\xi_{\mathcal{O}}$ is the noise operator. The coefficients $\gamma_{ij}^{(\mathrm{g})}$ and $\Omega_{ij}^{(\mathrm{g})}$ ($\gamma_{ij}^{(\mathrm{r})}$ and $\Omega_{ij}^{(\mathrm{r})}$) describe spontaneous emission into guided (radiation) modes. The decay coefficients $\gamma_{ij}^{(\mathrm{g})}$ and $\gamma_{ij}^{(\mathrm{r})}$ are

$$\gamma_{ij}^{(\mathrm{g})} = 2\pi \sum_{fp} G_{\mu_0 i} G_{\mu_0 j}^*,$$

$$\gamma_{ij}^{(\mathrm{r})} = 2\pi \sum_{mp} \int_{-k_0 n_2}^{k_0 n_2} d\beta\, G_{\nu_0 i} G_{\nu_0 j}^*, \quad (13)$$

where $\mu_0 = (\omega_0, f, p)$ and $\nu_0 = (\omega_0, \beta, m, p)$ label the resonant guided and radiation modes, respectively, whose frequencies coincide with the atomic frequency ω_0. The frequency shift coefficients $\Omega_{ij}^{(\mathrm{g})}$ and $\Omega_{ij}^{(\mathrm{r})}$ are

$$\Omega_{ij}^{(\mathrm{g})} = -\mathrm{P}\int_0^\infty d\omega \sum_{fp} \left(\frac{G_{\mu i} G_{\mu j}^*}{\omega - \omega_0} - (-1)^{i+j} \frac{G_{\mu i}^* G_{\mu j}}{\omega + \omega_0} \right),$$

$$\Omega_{ij}^{(\mathrm{r})} = -\mathrm{P}\int_0^\infty d\omega \sum_{mp} \int_{-kn_2}^{kn_2} d\beta \left(\frac{G_{\nu i} G_{\nu j}^*}{\omega - \omega_0} - (-1)^{i+j} \frac{G_{\nu i}^* G_{\nu j}}{\omega + \omega_0} \right). \quad (14)$$

Note that $\gamma_{ij} = \gamma_{ji}^*$ and $\Omega_{ij} = \Omega_{ji}^*$. In addition, we can show that $\gamma_{ij} = \gamma_{ij}^*$ and $\Omega_{ij} = \Omega_{ij}^*$ (see the discussions around the end of this section).

When we use the Heisenberg-Langevin equation (11) and the relation $\mathrm{Tr}[\mathcal{O}(t)\rho(0)] = \mathrm{Tr}[\mathcal{O}(0)\rho(t)]$, we find the master equation

$$\dot{\rho} = \frac{1}{2}\sum_{ij} \gamma_{ij}(2\sigma_j \rho \sigma_i^\dagger - \sigma_i^\dagger \sigma_j \rho - \rho \sigma_i^\dagger \sigma_j) - i\sum_{ij} \Omega_{ij}[\sigma_i^\dagger \sigma_j, \rho] \quad (15)$$

for the reduced density operator ρ of the atomic system. In deriving the above equation, we multiplied Eq. (11) with $\rho(0)$, took the trace of the result, changed from the picture for $\mathrm{Tr}[\mathcal{O}(t)\rho(0)]$ to the picture for $\mathrm{Tr}[\mathcal{O}(0)\rho(t)]$, transformed to arrange the operator $\mathcal{O}(0)$ at the first position in each operator product, and eliminated $\mathcal{O}(0)$.

The basic equations (11) and (15) are valid only in the framework of the Markov approximation. This approximation requires the atom-field correlation time to be short as compared to the characteristic decay time. Such a short memory is possible only when the mode spectrum is regular and broadband. When the atomic frequency is near to the cutoff frequency of the fiber, significant non-Markovian effects may appear due to the irregularity of the density of guided modes at the cutoff [27]. Therefore, for the validity of the Markov approximation, the atomic frequency should not be close to the cutoff frequency. The atom-field correlation may also be affected by the confinement of photons in guided modes, resulting from multiple reflections off the fiber surface [28], or by the energy exchange between the two atoms [26]. Therefore, if the atom-field coupling is strong, the Markov approximation may not work properly when the atoms are too close to each other or to the fiber surface. However, when the atom-field interaction is weak, the restrictions are less stringent. Another complication may appear when the atoms are positioned too close to the fiber surface. The abrupt change of the refractive index at the fiber surface leads to abrupt changes in mode functions, mode density, and decay characteristics. Such irregularities occur in the spatial dependence. They are different from the irregularity in the frequency dependency of the mode density at the edge of a photon band gap [27]. Although spatial irregularities do not affect the Markov approximation directly, they invalidate the macroscopic Maxwell equations at the surface. In order to describe this case, the whole theory for the atom-field interaction must be revised. Instead of the mean field and the continuous structure of the fiber, the local field and the discrete atomic structure of the material must be considered. However, this problem is beyond the scope of the present paper.

The diagonal coefficients $\gamma_{jj}^{(g)}$ and $\gamma_{jj}^{(r)}$ describe the spontaneous decay of the individual atoms into guided and radiation modes, respectively. When we set $i=j$ in Eqs. (13) and use the symmetry of the mode functions, we find

$$\gamma_{jj}^{(g)} = \frac{2\omega_0\beta_0'}{\epsilon_0\hbar}\sum_l d_{jl}^2 |e_l^{(0)}(r_j)|^2,$$

$$\gamma_{jj}^{(r)} = \frac{2\omega_0}{\epsilon_0\hbar}\sum_{lm} d_{jl}^2 \int_0^{k_0 n_2} d\beta |e_l^{(\beta m)}(r_j)|^2, \tag{16}$$

where the index l labels the r, φ, and z vector components, and $e_l^{(0)}$ and $e_l^{(\beta m)}$ are the resonant mode functions $e_l^{(\omega_0,f=+,p=+)}$ and $e_l^{(\omega_0,\beta,m,p=+)}$ of guided and radiation modes, respectively. It is clear that $\gamma_{jj}^{(g)}$, $\gamma_{jj}^{(r)}$, and consequently γ_{jj} are real parameters. The decay rates of single two-level atoms [18–20] and multilevel cesium atoms [17] have been studied in detail.

The off-diagonal coefficients $\gamma_{12}^{(g)}$ and $\gamma_{12}^{(r)}$ characterize the energy transfers between the atoms due to guided and radiation modes, respectively. When we set $i=1$ and $j=2$ in Eqs. (13) and use the symmetry of the mode functions, we find

$$\gamma_{12}^{(g)} = \frac{2\omega_0\beta_0'}{\epsilon_0\hbar}\sum_{l_1 l_2} d_{1l_1} d_{2l_2} U_{l_1 l_2}^{(g)},$$

$$\gamma_{12}^{(r)} = \frac{2\omega_0}{\epsilon_0\hbar}\sum_{l_1 l_2} d_{1l_1} d_{2l_2} U_{l_1 l_2}^{(r)}, \tag{17}$$

where

$$\begin{aligned}
U_{ll}^{(g)} &= e_l^{(0)}(r_1) e_l^{(0)*}(r_2)\cos(\varphi_1-\varphi_2)\cos\beta_0(z_1-z_2),\\
U_{r\varphi}^{(g)} &= i e_r^{(0)}(r_1) e_\varphi^{(0)*}(r_2)\sin(\varphi_1-\varphi_2)\cos\beta_0(z_1-z_2),\\
U_{zr}^{(g)} &= i e_z^{(0)}(r_1) e_r^{(0)*}(r_2)\cos(\varphi_1-\varphi_2)\sin\beta_0(z_1-z_2),\\
U_{z\varphi}^{(g)} &= -e_z^{(0)}(r_1) e_\varphi^{(0)*}(r_2)\sin(\varphi_1-\varphi_2)\sin\beta_0(z_1-z_2),
\end{aligned} \tag{18}$$

and

$$\begin{aligned}
U_{ll}^{(r)} &= \sum_m \int_0^{k_0 n_2} d\beta\, e_l^{(\beta m)}(r_1) e_l^{(\beta m)*}(r_2)\\
&\quad\times\cos m(\varphi_1-\varphi_2)\cos\beta(z_1-z_2),\\
U_{r\varphi}^{(r)} &= i\sum_m \int_0^{k_0 n_2} d\beta\, e_r^{(\beta m)}(r_1) e_\varphi^{(\beta m)*}(r_2)\\
&\quad\times\sin m(\varphi_1-\varphi_2)\cos\beta(z_1-z_2),\\
U_{zr}^{(r)} &= i\sum_m \int_0^{k_0 n_2} d\beta\, e_z^{(\beta m)}(r_1) e_r^{(\beta m)*}(r_2)\\
&\quad\times\cos m(\varphi_1-\varphi_2)\sin\beta(z_1-z_2),\\
U_{z\varphi}^{(r)} &= -\sum_m \int_0^{k_0 n_2} d\beta\, e_z^{(\beta m)}(r_1) e_\varphi^{(\beta m)*}(r_2)\\
&\quad\times\sin m(\varphi_1-\varphi_2)\sin\beta(z_1-z_2).
\end{aligned} \tag{19}$$

The subscripts l_1, l_2, and l in Eqs. (17)–(19) label the r, φ, or z orientation of the atomic dipoles. Note that, due to the relations (A9) and (B9), all the coefficients $U_{l_1 l_2}^{(g)}$ and $U_{l_1 l_2}^{(r)}$ are real parameters, and so are the cross-decay rates $\gamma_{12}^{(g)}$, $\gamma_{12}^{(r)}$, and γ_{12}.

According to Eqs. (18), the z dependences of the coefficients $U_{l_1 l_2}^{(g)}$ are described by the trigonometric functions $\cos\beta_0(z_1-z_2)$ and $\sin\beta_0(z_1-z_2)$. Due to this property, the cross coefficient due to guided modes $\gamma_{12}^{(g)}$ is periodic in the z direction with the period $2\pi/\beta_0$ and, consequently, does not reduce to zero with increasing z_1-z_2. Meanwhile, due to the integration over β in Eqs. (19), the cross coefficient due to radiation modes $\gamma_{12}^{(r)}$ reduces to zero with increasing z_1-z_2. Therefore, the total cross-decay coefficient γ_{12} may remain substantial for large distances between the atoms. In the limit of large $|z_2-z_1|$, the total coefficient γ_{12} is mainly determined by $\gamma_{12}^{(g)}$ and is quasiperiodic with the period $2\pi/\beta_0$.

The diagonal coefficients Ω_{11} and Ω_{22} describe the Lamb shifts of the first and second atoms, respectively, in the presence of the fiber. They must be renormalized. Their renormalized magnitudes are typically small as compared to the optical frequency ω_0 of the atoms. The cross coefficient Ω_{12} characterizes the energy of the dipole-dipole interaction between the atoms. This coefficient is typically small as compared to ω_0 when the atomic separation $|\mathbf{r}_1-\mathbf{r}_2|$ is larger than the optical wavelength $\lambda_0=2\pi c/\omega_0$. The components $\Omega_{12}^{(g)}$ and $\Omega_{12}^{(r)}$ correspond to the contributions of guided and radiation modes, respectively. The explicit expressions for $\Omega_{12}^{(g)}$ and $\Omega_{12}^{(r)}$ are given in Appendix C. It can be shown that $\Omega_{12}^{(g)}$ and $\Omega_{12}^{(r)}$ are real parameters and decrease to zero with increasing $|z_2-z_1|$. Consequently, in the limit of large $|z_2-z_1|$, the cross-frequency-shift coefficient Ω_{12} can be neglected, as in the case of two atoms in free space.

IV. TWO-ATOM DYNAMICS

In order to get insight into collective spontaneous decay of two distant atoms in the vicinity of a fiber, we try to get some simple analytical results. We note that the Lamb shifts are usually small. The frequency shifts caused by the dipole-dipole interaction are also small when the separation between the atoms is large. For simplicity, we neglect the Lamb shifts as well as the frequency shifts caused by the dipole-dipole interaction. Then, Eq. (11) for the atomic operator $\mathcal{O}$ reduces to

$$\dot{\mathcal{O}} = \frac{1}{2}\sum_{i,j=1}^{2} \gamma_{ij}([\sigma_i^\dagger,\mathcal{O}]\sigma_j + \sigma_i^\dagger[\mathcal{O},\sigma_j]) + \xi_{\mathcal{O}}. \tag{20}$$

Similarly, Eq. (15) for the reduced density operator ρ of the atoms reduces to

$$\dot{\rho} = \frac{1}{2}\sum_{i,j=1}^{2} \gamma_{ij}(2\sigma_j\rho\sigma_i^\dagger - \sigma_i^\dagger\sigma_j\rho - \rho\sigma_i^\dagger\sigma_j). \tag{21}$$

A. Decay of the total excited population

From Eq. (20), we find the following closed set of equations:

$$\frac{d}{dt}\sigma_{z1} = -\gamma_{11}(\sigma_{z1}+1) - \gamma_{12}(\sigma_1^\dagger\sigma_2 + \sigma_2^\dagger\sigma_1) + \xi_{z1},$$

$$\frac{d}{dt}\sigma_{z2} = -\gamma_{22}(\sigma_{z2}+1) - \gamma_{12}(\sigma_1^\dagger\sigma_2 + \sigma_2^\dagger\sigma_1) + \xi_{z2},$$

$$\frac{d}{dt}\sigma_1^\dagger\sigma_2 = -\frac{1}{2}(\gamma_{11}+\gamma_{22})\sigma_1^\dagger\sigma_2 + \frac{1}{4}\gamma_{12}(\sigma_{z1}+\sigma_{z2}+2\sigma_{z1}\sigma_{z2}) + \xi_{12},$$

$$\frac{d}{dt}\sigma_2^\dagger\sigma_1 = -\frac{1}{2}(\gamma_{11}+\gamma_{22})\sigma_2^\dagger\sigma_1 + \frac{1}{4}\gamma_{12}(\sigma_{z1}+\sigma_{z2}+2\sigma_{z1}\sigma_{z2}) + \xi_{12}^\dagger,$$

$$\frac{d}{dt}\sigma_{z1}\sigma_{z2} = -\gamma_{11}\sigma_{z2} - \gamma_{22}\sigma_{z1} - (\gamma_{11}+\gamma_{22})\sigma_{z1}\sigma_{z2} + 2\gamma_{12}(\sigma_1^\dagger\sigma_2 + \sigma_2^\dagger\sigma_1) + \xi_{zz}. \tag{22}$$

We introduce the variable

$$P = \frac{\langle\sigma_{z1}\rangle+1}{2} + \frac{\langle\sigma_{z2}\rangle+1}{2} = \langle\sigma_{e1e1}\rangle + \langle\sigma_{e2e2}\rangle, \tag{23}$$

which describes the total population of the excited levels $|e_1\rangle$ and $|e_2\rangle$ of the two atoms. We note that the variation of P is equal to the variation of the photon number. Therefore, the rate of decay of P is the rate of collective spontaneous emission of the two atoms. The variable P together with the two other variables

$$V = \frac{\Delta}{2\gamma_a}(\langle\sigma_{z1}\rangle - \langle\sigma_{z2}\rangle) + \frac{\gamma_{12}}{\gamma_a}(\langle\sigma_1^\dagger\sigma_2\rangle + \langle\sigma_2^\dagger\sigma_1\rangle),$$

$$Z = \langle\sigma_{z1}\sigma_{z2}\rangle - 1 \tag{24}$$

are governed by the following closed set of equations:

$$\dot{P} = -\gamma_a(P+V),$$

$$\dot{V} = -\gamma_a V + \frac{\gamma_{12}^2-\Delta^2}{\gamma_a}P + \frac{\gamma_{12}^2}{\gamma_a}Z,$$

$$\dot{Z} = -2\gamma_a(Z+P-V). \tag{25}$$

Here we have introduced the notation

$$\gamma_a = (\gamma_{11}+\gamma_{22})/2, \quad \Delta = (\gamma_{11}-\gamma_{22})/2. \tag{26}$$

The eigenvalues of the characteristic matrix for the differential equations (25) are $2\gamma_a$, γ^+, and γ^-, where

$$\gamma^\pm = \gamma_a \pm \sqrt{\gamma_{12}^2+\Delta^2}. \tag{27}$$

Therefore, the general expression for the total excited population P can be written in the form

$$P = \mathcal{A}e^{-2\gamma_a t} + \mathcal{A}^+e^{-\gamma^+ t} + \mathcal{A}^-e^{-\gamma^- t}, \tag{28}$$

where the coefficients $\mathcal{A}$, $\mathcal{A}^+$, and $\mathcal{A}^-$ are determined by the initial conditions. We can show that $\gamma_a \geqslant \sqrt{\gamma_{11}\gamma_{22}} \geqslant |\gamma_{12}|$ and hence $\gamma^\pm \geqslant 0$. The eigenvalue $2\gamma_a$ is the decay rate of the fully excited state $|ee\rangle = |e_1\rangle \otimes |e_2\rangle$. The eigenvalues γ^+ and γ^- are the decay rates of the superradiant state $|+\rangle$ and the subradiant state $|-\rangle$, respectively. The explicit expressions for the states $|+\rangle$ and $|-\rangle$ and for the total excited population P will be given in the next subsection.

B. Superradiant and subradiant states

We introduce the two-atom basis states [see Fig. 1(c)]

$$|u\rangle = |ee\rangle, \quad |b\rangle = |gg\rangle, \tag{29}$$

and

$$|+\rangle = \cos\theta|eg\rangle + \sin\theta|ge\rangle, \quad |-\rangle = -\sin\theta|eg\rangle + \cos\theta|ge\rangle, \tag{30}$$

where θ is determined by the equations

$$\sin 2\theta = \frac{\gamma_{12}}{\sqrt{\gamma_{12}^2+\Delta^2}}, \quad \cos 2\theta = \frac{\Delta}{\sqrt{\gamma_{12}^2+\Delta^2}}. \tag{31}$$

In this basis, we find from Eq. (21) that the equations for the diagonal matrix elements form a closed set

$$\dot{\rho}_{uu} = -2\gamma_a\rho_{uu}, \quad \dot{\rho}_{++} = \kappa^+\rho_{uu} - \gamma^+\rho_{++},$$

$$\dot{\rho}_{--} = \kappa^-\rho_{uu} - \gamma^-\rho_{--}, \quad \dot{\rho}_{bb} = \gamma^+\rho_{++} + \gamma^-\rho_{--}. \tag{32}$$

Here we have introduced the notation

$$\kappa^\pm = \gamma_a \pm \frac{\gamma_{12}^2-\Delta^2}{\sqrt{\gamma_{12}^2+\Delta^2}}. \tag{33}$$

Note that $\kappa^\pm \geqslant 0$ and $\kappa^+ + \kappa^- = 2\gamma_a$. According to Eqs. (32), the time evolution of the diagonal elements of ρ in the basis $\{|u\rangle, |b\rangle, |+\rangle, |-\rangle\}$ is decoupled from the off-diagonal elements. Consequently, Eqs. (32) are rate equations. As seen, the fully excited state $|u\rangle$ decays to the states $|+\rangle$ and $|-\rangle$ with the rates κ^+ and κ^-, respectively. The total decay rate of $|u\rangle$ is $\kappa^+ + \kappa^- = 2\gamma_a$. The states $|+\rangle$ and $|-\rangle$ decay to the two-atom ground state $|b\rangle$ with the rates γ^+ and γ^-, respectively. When $\gamma_{12} \neq 0$, the states $|+\rangle$ and $|-\rangle$ are entangled states of two atoms. The cross decay leads to an increase in the decay rate of the state $|+\rangle$ and a decrease in the decay rate of the state $|-\rangle$. The states $|+\rangle$ and $|-\rangle$ are superradiant and subradiant states, respectively, and are analogies of bright and dark states, respectively [29,30]. Note that, when $\gamma_{12} > 0$, the weight factors $\cos\theta$ and $\sin\theta$ have the same signs, indicating that the superradiant (subradiant) state $|+\rangle$ ($|-\rangle$) is a phased (antiphased) superposition of the bare states $|eg\rangle$ and $|ge\rangle$. However, when $\gamma_{12} < 0$, the weight factors $\cos\theta$ and $\sin\theta$ have opposite signs, indicating that the superradiant (subradiant) state is an antiphased (phased) superposition of the bare states.

We solve Eqs. (32) analytically. Then, we find for the populations of the states $|+\rangle$, $|-\rangle$, and $|u\rangle$ the expressions

$$\rho_{uu} = \rho_{uu}(0)e^{-2\gamma_a t},$$

$$\rho_{++} = -\frac{\kappa^+}{\gamma^-}\rho_{uu}(0)e^{-2\gamma_a t} + \left(\rho_{++}(0) + \frac{\kappa^+}{\gamma^-}\rho_{uu}(0)\right)e^{-\gamma^+ t},$$

$$\rho_{--} = -\frac{\kappa^-}{\gamma^+}\rho_{uu}(0)e^{-2\gamma_a t} + \left(\rho_{--}(0) + \frac{\kappa^-}{\gamma^+}\rho_{uu}(0)\right)e^{-\gamma^- t}. \tag{34}$$

The population of the two-atom ground state $|b\rangle$ is given by $\rho_{bb}=1-\rho_{uu}-\rho_{++}-\rho_{--}$. The total excited population is $P=2\rho_{uu}+\rho_{++}+\rho_{--}$. Using Eqs. (34), we find

$$P = -\frac{4\gamma_{12}^2}{\gamma^+\gamma^-}\rho_{uu}(0)e^{-2\gamma_a t} + \left(\rho_{++}(0) + \frac{\kappa^+}{\gamma^-}\rho_{uu}(0)\right)e^{-\gamma^+ t} + \left(\rho_{--}(0) + \frac{\kappa^-}{\gamma^+}\rho_{uu}(0)\right)e^{-\gamma^- t}. \tag{35}$$

When the two atoms are initially prepared in the superradiant state $|+\rangle$ or the subradiant state $|-\rangle$, we obtain $P=e^{-\gamma^+ t}$ or $P=e^{-\gamma^- t}$, respectively. When the atoms are initially prepared in the fully excited state $|u\rangle$, we obtain $P=-(4\gamma_{12}^2/\gamma^+\gamma^-)e^{-2\gamma_a t}+(\kappa^+/\gamma^-)e^{-\gamma^+ t}+(\kappa^-/\gamma^+)e^{-\gamma^- t}$.

We note that, in the case where $\gamma_{11}=\gamma_{22}=\gamma_a$ (i.e., $\Delta=0$) and $\gamma_{12}\neq 0$, expressions (30) for the superradiant and subradiant states $|+\rangle$ and $|-\rangle$ reduce to

$$|+\rangle = \frac{|eg\rangle + \mathrm{sgn}(\gamma_{12})|ge\rangle}{\sqrt{2}},$$

$$|-\rangle = \frac{-\mathrm{sgn}(\gamma_{12})|eg\rangle + |ge\rangle}{\sqrt{2}}, \tag{36}$$

with the decay rates

$$\gamma^+ = \kappa^+ = \gamma_a + |\gamma_{12}|,$$

$$\gamma^- = \kappa^- = \gamma_a - |\gamma_{12}|. \tag{37}$$

Here we have introduced the function $\mathrm{sgn}(x)=1$ or -1 for $x>0$ or <0, respectively. In this case, if γ_{12} is positive, the superradiant (subradiant) state $|+\rangle$ ($|-\rangle$) is the symmetric (antisymmetric) superposition of the bare states $|eg\rangle$ and $|ge\rangle$. However, if γ_{12} is negative, the superradiant (subradiant) state is the antisymmetric (symmetric) superposition of the bare states. Thus, both the superradiant state and the subradiant state can be a symmetric or antisymmetric superposition depending on the sign of the cross-decay rate γ_{12} and, consequently, on the relative placement of the atoms.

V. NUMERICAL CALCULATIONS

In what follows, we present the results of our numerical calculations pertaining to the cross-decay rate γ_{12} for various different mutual orientations of the atoms and their relative positions. For all of our calculations we take the fiber radius to be $a=200$ nm and the wavelength of the atomic transition to be $\lambda_0=852$ nm. The refractive indices of the fiber and the surrounding vacuum are $n_1=1.45$ and $n_2=1$, respectively. All the decay rates are normalized to the decay rate $\gamma_0=\omega_0^3 d^2/(3\pi\hbar\epsilon_0 c^3)$ of a single atom in free space, where $d=|\mathbf{d}_j|$.

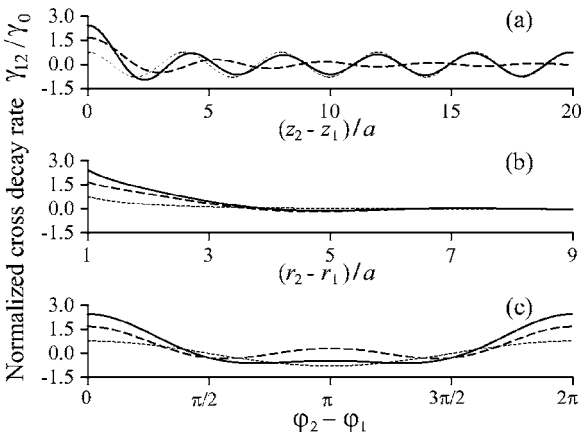

FIG. 2. Cross-decay rate γ_{12} (solid lines), normalized to the free-space spontaneous decay rate γ_0, as a function of (a) the axial, (b) radial, and (c) angular separations between two atoms. The position of the first atom is fixed at $r_1=a$, $\varphi_1=0$, and $z_1=0$. One coordinate of the second atom is varied, while the two others are fixed as (a) $r_2=a$ and $\varphi_2=0$, (b) $\varphi_2=0$ and $z_2=0$, and (c) $r_2=a$ and $z_2=0$. The contribution from guided (radiation) modes is shown by dotted (dashed) lines. The dipoles of both the atoms are *r* oriented.

The results for both the atoms having the same radial orientation (hereafter referred to as *r*-oriented atoms) are shown in Fig. 2, where the dotted, dashed, and solid curves refer to the cross-decay rates due to the guided modes, the radiation modes, and the cumulative effect (sum of the two rates) of these modes, respectively. It can be easily discerned from Fig. 2(a) that the effect of guided modes persists over arbitrarily large axial separations between the atoms while that due to the radiation modes decays to zero. Thus the guided modes of the fiber play a crucial role in maintaining the exchange over large distances. Such long-distance interaction cannot exist in free space. The periodicity of the cross-decay rate into guided modes [see the dotted curve in Fig. 2(a)] is a direct consequence of the trigonometric functions $\cos\beta_0(z_1-z_2)$ and $\sin\beta_0(z_1-z_2)$ in Eqs. (18). The varying oscillation period and the reduction in magnitude in the case of radiation modes [see the dashed curve in Fig. 2(a)] can be attributed to the effect of the integrals of the trigonometric functions in Eqs. (19). It is thus clear that one can control the exchange between the atoms by varying the separation between them with maximum exchange at certain locations. Another point that deserves attention is the possibility of the decay channels due to guided and radiation modes to act out of phase and consequently to compensate each other. Figure 2(b) illustrates how the cross-decay rate decreases as one increases the radial distance between the atoms. Figure 2(c) gives the variation of the cross-decay rate as the azimuthal angle is varied. As seen, the cross-decay rate is extremely sensitive to the mutual orientations and the placements of the two atoms.

In order to further demonstrate the sensitivity of the cross-decay rate γ_{12} to the mutual orientations and relative posi-

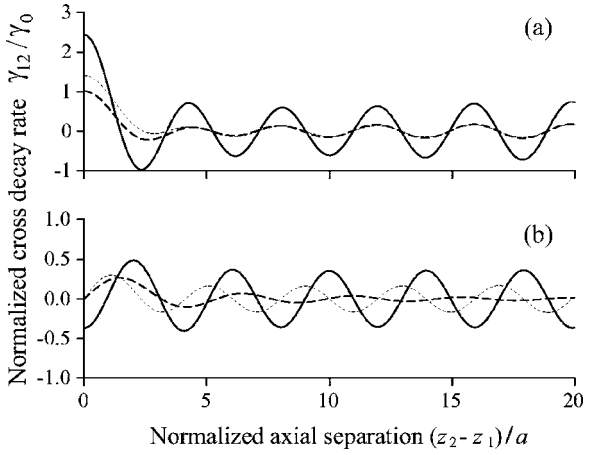

FIG. 3. Cross-decay rate γ_{12}, normalized to the free-space spontaneous decay rate γ_0, as a function of the axial angular separation between two atoms with (a) the same and (b) different dipole-moment orientations. In (a), the solid, dashed, and dotted lines correspond to the common r, φ, and z orientations, respectively. In (b), the solid, dashed, and dotted lines correspond to the pairs of r and φ, z and r, and z and φ orientations, respectively. The position of the first atom is fixed at $r_1=a$, $\varphi_1=0$, and $z_1=0$. The axial coordinate of the second atom is varied while the two others are fixed as $r_2=a$ and $\varphi_2=0$ (a) or $\pi/2$ (b).

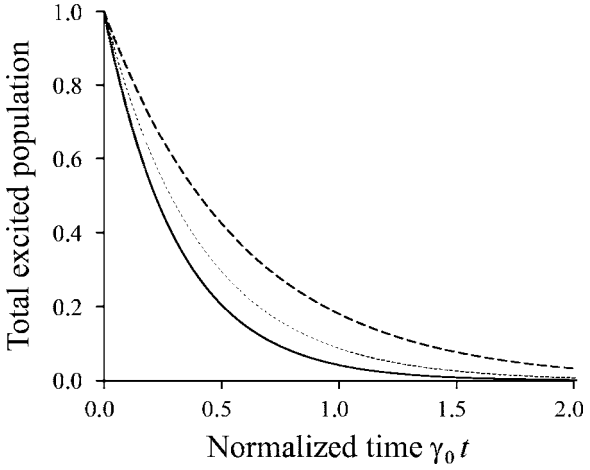

FIG. 4. Decay of the total upper-state population of two atoms with a single initial excitation in the vicinity of a thin fiber. The atoms are initially prepared in the superradiant $|+\rangle$ (solid line) or the subradiant $|-\rangle$ (dashed line) state. The coordinates of the atoms are $r_1=r_2=a$, $\varphi_1=\varphi_2=0$, and $(z_2-z_1)/a=20$. Both the atomic dipoles are r oriented. For comparison, the decay of the upper-state population of a single atom with the rate γ_a is shown by the dotted line.

tions of the atoms we show this rate in Fig. 3 as a function of the normalized distance $(z_2-z_1)/a$ for various mutual orientations of the atoms. Figure 3(a) gives the results for identical orientations of the dipole moments. Figure 3(b) gives the results for nonidentical orientations. The overall behavior in Fig. 3 reflects the oscillations in both guided and radiation components as well as the reduction in magnitude of the radiation component. The comparison between the vertical scales of Figs. 3(a) and 3(b) shows the reduction of exchange for nonidentical orientations of the dipoles. The strongest cross talk occurs for both the dipoles having the same r orientation.

We next look at the temporal evolution of the total excited population $P=\langle\sigma_{e_1e_1}\rangle+\langle\sigma_{e_2e_2}\rangle$ when the system is initially prepared in the superradiant state $|+\rangle$ or the subradiant state $|-\rangle$. The results for $r_1=r_2=a$ (the atoms are on the fiber surface) and $\varphi_1=\varphi_2=0$, with a large axial separation between the atoms, namely, $(z_2-z_1)/a=20$, are shown in Fig. 4. Both the atomic dipoles are assumed to be r oriented. The figure shows that the decay of the total population of the two atoms depends crucially on the initial state of the system. Indeed, the decay is faster for the superradiance case (solid line) and slower for the subradiance case (dashed line) [22,23,31]. The most noteworthy feature is the persistence of the significant collective effect over large distances. As is clear from the earlier data (Figs. 2 and 3) on cross-decay rates, the role of the radiation modes over such distances is comparatively negligible. The cooperation between the atoms, observed in Fig. 4, is mediated basically by the guided modes and can survive over large distances.

To get deeper insight into the effect of the fiber on the collective decay of two distant atoms, we plot in Fig. 5 the superradiant decay rate γ^+, the subradiant decay rate γ^-, and the averaged single-atom decay rate γ_a as functions of the radial distance r for the parameters $r_1=r_2=r$, $\varphi_1=\varphi_2=0$, and $(z_2-z_1)/a=20$. Both the atomic dipoles are assumed to be r oriented. The figure shows that, when the atoms are on the fiber surface, the subradiant decay rate is about 54% of the superradiant decay rate and is about 70% of the single-atom decay rate. The differences between γ^+, γ^-, and γ_a are substantial although the atomic separation $|\mathbf{r}_2-\mathbf{r}_1|=|z_2-z_1|=4$ μm is large as compared to the atomic transition wavelength $\lambda_0=852$ nm. Such substantial differences are mainly caused by the contribution $\gamma_{12}^{(g)}$ of guided modes. The effect of the fiber on the differences between γ^+, γ^-, and γ_a quickly reduces with increasing radial distance r. Due to the periodicity of $\gamma_{12}^{(g)}$, the rates γ^+ and γ^- are quasiperiodic in the z direction with the period $2\pi/\beta_0$.

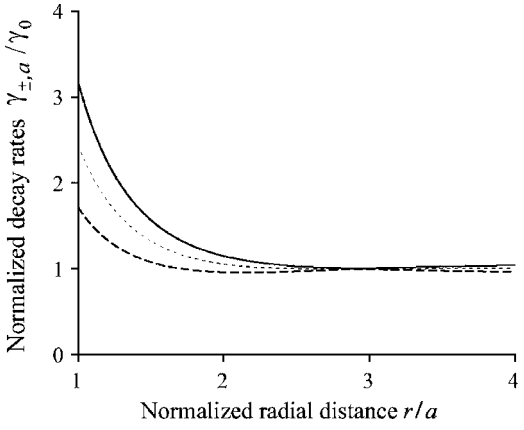

FIG. 5. Decay rates γ^+ (solid line), γ^- (dashed line), and γ_a (dotted line), normalized to the free-space spontaneous decay rate γ_0, as functions of the radial distance r. The coordinates of the atoms are $r_1=r_2=r$, $\varphi_1=\varphi_2=0$, and $(z_2-z_1)/a=20$. Both the atomic dipoles are r oriented.

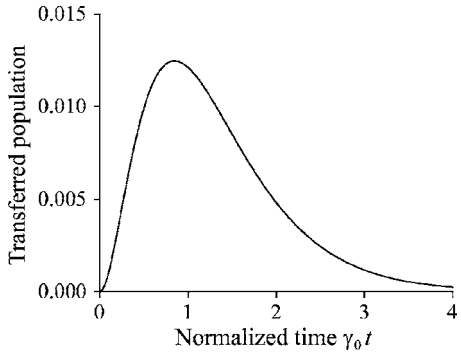

FIG. 6. Time evolution of the population of the second atom transferred from the first atom. At the initial time, the first atom is excited, while the second atom is in the ground state. The coordinates of the atoms are $r_1=r_2=a$, $\varphi_1=\varphi_2=0$, and $(z_2-z_1)/a=20$. Both the atomic dipoles are r oriented.

Finally, we demonstrate the transfer of energy between two distant atoms in the vicinity of the fiber. We solve Eqs. (22) numerically for the case where the first atom is initially in the excited state $|e_1\rangle$ while the second atom is initially in the ground state $|g_2\rangle$. We use this solution to calculate the excited population (energy) $\langle\sigma_{e_2e_2}\rangle=(\langle\sigma_{z2}\rangle+1)/2$ of the second atom as a function of time. The results for $r_1=r_2=a$ (the atoms are on the fiber surface) and $\varphi_1=\varphi_2=0$, with a large axial separation between the atoms, namely, $(z_2-z_1)/a=20$, are shown in Fig. 6. Both the atomic dipoles are assumed to be r oriented. The figure shows that the excited population of the second atom quickly builds up and then slowly decays. The peak value is 0.0125, reached at the time $t=0.84\gamma_0^{-1}$. Thus, 1.25% of the energy of the first atom can be transferred to the second atom even though the separation between the atoms is large as compared to the atomic transition wavelength. Due to the periodicity of $\gamma_{12}^{(g)}$, the magnitude of the transferred energy does not change much when the axial separation $|z_2-z_1|$ between the atoms is increased by an integer multiple of $2\pi/\beta_0$.

VI. SUMMARY

In conclusion, we have studied resonant dipole-dipole interaction near a nanofiber with full account of the radiation and guided modes. The formulation is general, applicable to arbitrary placements and orientations of the atomic dipoles. We have presented the numerical results for the cross-decay rate for typical choices of the orientations of the dipoles and their locations. At large distances between the dipoles, the effect of the radiation modes is shown to be negligible, while a substantial exchange survives due to the guided modes. We have shown that the interaction is extremely sensitive to the mutual placements and orientations of the dipoles and thus can be controlled by a suitable design of the microscopic traps. The exchange between the atoms is shown to be particularly important for radially oriented dipoles near the fiber surface and parallel to the fiber axis. This interaction is shown to lead to a substantially smaller decay rate for the subradiant state as compared to the superradiant state and to the single-atom excited state even though the two atoms are distant from each other. We have demonstrated that a substantial amount of energy can be transferred from an atom to a distant atom via guided modes. We believe that the longevity of subradiant entangled states as well as the substantial energy transfer mediated by the nanofiber over large distances can find important applications in quantum information and quantum computing.

ACKNOWLEDGMENTS

This work was carried out under the 21st Century COE program on "Coherent Optical Science."

APPENDIX A: MODE FUNCTIONS OF THE FUNDAMENTAL GUIDED MODES

For the guided modes, the propagation constant β is determined by the fiber eigenvalue equation [25]

$$\frac{J_0(ha)}{haJ_1(ha)}=-\frac{n_1^2+n_2^2}{2n_1^2}\frac{K_1'(qa)}{qaK_1(qa)}+\frac{1}{h^2a^2}-\left[\left(\frac{n_1^2-n_2^2}{2n_1^2}\frac{K_1'(qa)}{qaK_1(qa)}\right)^2+\frac{\beta^2}{n_1^2k^2}\left(\frac{1}{q^2a^2}+\frac{1}{h^2a^2}\right)^2\right]^{1/2}. \tag{A1}$$

Here the parameters $h=(n_1^2k^2-\beta^2)^{1/2}$ and $q=(\beta^2-n_2^2k^2)^{1/2}$ characterize the fields inside and outside the fiber, respectively. The notation J_n and K_n stand for the Bessel functions of the first kind and the modified Bessel functions of the second kind, respectively.

The mode functions of the electric parts of the fundamental guided modes [25] are given, for $r<a$, by

$$e_r^{(\mu)}=iA\frac{q}{h}\frac{K_1(qa)}{J_1(ha)}[(1-s)J_0(hr)-(1+s)J_2(hr)],$$

$$e_\varphi^{(\mu)}=-pA\frac{q}{h}\frac{K_1(qa)}{J_1(ha)}[(1-s)J_0(hr)+(1+s)J_2(hr)],$$

$$e_z^{(\mu)}=fA\frac{2q}{\beta}\frac{K_1(qa)}{J_1(ha)}J_1(hr), \tag{A2}$$

and, for $r>a$, by

$$e_r^{(\mu)}=iA[(1-s)K_0(qr)+(1+s)K_2(qr)],$$

$$e_\varphi^{(\mu)}=-pA[(1-s)K_0(qr)-(1+s)K_2(qr)],$$

$$e_z^{(\mu)}=fA\frac{2q}{\beta}K_1(qr). \tag{A3}$$

Here the parameter s is defined as $s=(1/q^2a^2+1/h^2a^2)/[J_1'(ha)/haJ_1(ha)+K_1'(qa)/qaK_1(qa)]$, and the coefficient A is determined from the normalization condition.

To normalize the guided mode functions, we need to calculate the constant

$$N_\mu = \int_0^{2\pi} d\varphi \int_0^\infty n_{\rm rf}^2 |\mathbf{e}^{(\mu)}|^2 r\, dr. \tag{A4}$$

We find

$$N_\mu = 2\pi |A|^2 a^2 (n_1^2 P_1 + n_2^2 P_2), \tag{A5}$$

where

$$P_1 = \frac{q^2 K_1^2(qa)}{h^2 J_1^2(ha)} \Bigg((1-s)^2 [J_0^2(ha) + J_1^2(ha)] + (1+s)^2 [J_2^2(ha) - J_1(ha) J_3(ha)] + 2\frac{h^2}{\beta^2} [J_1^2(ha) - J_0(ha) J_2(ha)] \Bigg) \tag{A6}$$

and

$$P_2 = (1-s)^2 [K_1^2(qa) - K_0^2(qa)] + (1+s)^2 [K_1(qa) K_3(qa) - K_2^2(qa)] + 2\frac{q^2}{\beta^2} [K_0(qa) K_2(qa) - K_1^2(qa)]. \tag{A7}$$

In the case where the coefficient A is real, we have the following symmetry relations:

$$e_r^{(\omega,f,p)} = e_r^{(\omega,-f,p)} = e_r^{(\omega,f,-p)},$$

$$e_\varphi^{(\omega,f,p)} = e_\varphi^{(\omega,-f,p)} = -e_\varphi^{(\omega,f,-p)},$$

$$e_z^{(\omega,f,p)} = -e_z^{(\omega,-f,p)} = e_z^{(\omega,f,-p)}, \tag{A8}$$

and

$$e_r^{(\mu)*} = -e_r^{(\mu)}, \quad e_\varphi^{(\mu)*} = e_\varphi^{(\mu)}, \quad e_z^{(\mu)*} = e_z^{(\mu)}. \tag{A9}$$

APPENDIX B: MODE FUNCTIONS OF THE RADIATION MODES

For the radiation modes, we have $-kn_2 < \beta < kn_2$. The characteristic parameters for the field in the inside and outside of the fiber are $h = \sqrt{k^2 n_1^2 - \beta^2}$ and $q = \sqrt{k^2 n_2^2 - \beta^2}$, respectively. The mode functions of the electric parts of the radiation modes [25] are given, for $r < a$, by

$$e_r^{(\nu)} = \frac{i}{h^2} \Bigg(\beta h A J_m'(hr) + im \frac{\omega \mu_0}{r} B J_m(hr) \Bigg),$$

$$e_\varphi^{(\nu)} = \frac{i}{h^2} \Bigg(im \frac{\beta}{r} A J_m(hr) - h\omega\mu_0 B J_m'(hr) \Bigg),$$

$$e_z^{(\nu)} = A J_m(hr), \tag{B1}$$

and, for $r > a$, by

$$e_r^{(\nu)} = \frac{i}{q^2} \sum_{j=1,2} \Bigg(\beta q C_j H_m^{(j)\prime}(qr) + im \frac{\omega\mu_0}{r} D_j H_m^{(j)}(qr) \Bigg),$$

$$e_\varphi^{(\nu)} = \frac{i}{q^2} \sum_{j=1,2} \Bigg(im \frac{\beta}{r} C_j H_m^{(j)}(qr) - q\omega\mu_0 D_j H_m^{(j)\prime}(qr) \Bigg),$$

$$e_z^{(\nu)} = \sum_{j=1,2} C_j H_m^{(j)}(qr). \tag{B2}$$

The coefficients C_j and D_j are related to the coefficients A and B as [18]

$$C_j = (-1)^j \frac{i\pi q^2 a}{4 n_2^2} (A L_j + i\mu_0 c B V_j),$$

$$D_j = (-1)^{j-1} \frac{i\pi q^2 a}{4} (i\epsilon_0 c A V_j - B M_j), \tag{B3}$$

where

$$V_j = \frac{mk\beta}{a h^2 q^2} (n_2^2 - n_1^2) J_m(ha) H_m^{(j)*}(qa),$$

$$M_j = \frac{1}{h} J_m'(ha) H_m^{(j)*}(qa) - \frac{1}{q} J_m(ha) H_m^{(j)*\prime}(qa),$$

$$L_j = \frac{n_1^2}{h} J_m'(ha) H_m^{(j)*}(qa) - \frac{n_2^2}{q} J_m(ha) H_m^{(j)*\prime}(qa). \tag{B4}$$

Note that $V_1 = V_2^*$, $M_1 = M_2^*$, and $L_1 = L_2^*$. In addition, we have $C_1/A = (C_2/A)^*$ and $D_1/A = -(D_2/A)^*$. We specify two polarizations by choosing $B = i\eta A$ or $B = -i\eta A$ for $p = +$ and $p = -$, respectively. The orthogonality of the modes requires

$$\int_0^{2\pi} d\varphi \int_0^\infty n_{\rm rf}^2 [\mathbf{e}^{(\nu)} \mathbf{e}^{(\nu')*}]_{\beta=\beta', m=m'} r\, dr = N_\nu \delta_{pp'} \delta(\omega - \omega'). \tag{B5}$$

This leads to

$$\eta = \epsilon_0 c \sqrt{\frac{n_2^2 |V_j|^2 + |L_j|^2}{|V_j|^2 + n_2^2 |M_j|^2}}. \tag{B6}$$

The normalization factor N_ν is given by

$$N_\nu = \frac{8\pi\omega}{q^2} \Bigg(n_2^2 |C_j|^2 + \frac{\mu_0}{\epsilon_0} |D_j|^2 \Bigg). \tag{B7}$$

In the case where A is real, we have the following symmetry relations:

$$e_r^{(\omega,\beta,m,p)} = -e_r^{(\omega,-\beta,m,-p)},$$

$$e_\varphi^{(\omega,\beta,m,p)} = -e_\varphi^{(\omega,-\beta,m,-p)},$$

$$e_z^{(\omega,\beta,m,p)} = e_z^{(\omega,-\beta,m,-p)},$$

$$e_{r,\varphi,z}^{(\omega,\beta,m,p)} = (-1)^m e_{r,\varphi,z}^{(\omega,-\beta,-m,p)*}, \tag{B8}$$

and

$$e_r^{(\nu)*} = -e_r^{(\nu)}, \quad e_\varphi^{(\nu)*} = e_\varphi^{(\nu)}, \quad e_z^{(\nu)*} = e_z^{(\nu)}. \tag{B9}$$

APPENDIX C: CROSS-FREQUENCY SHIFTS

The coefficients $\Omega_{12}^{(\rm g)}$ and $\Omega_{12}^{(\rm r)}$ are the contributions of guided and radiation modes, respectively, to the cross coef-

ficient Ω_{12}, which characterizes the energy of the dipole-dipole interaction. From Eqs. (14) and (7), we find

$$\Omega_{12}^{(g)} = \frac{1}{\epsilon_0 \hbar} \sum_{l_1 l_2} d_{1l_1} d_{2l_2} W_{l_1 l_2}^{(g)},$$

$$\Omega_{12}^{(r)} = \frac{1}{\epsilon_0 \hbar} \sum_{l_1 l_2} d_{1l_1} d_{2l_2} W_{l_1 l_2}^{(r)}, \tag{C1}$$

where

$$W_{ll}^{(g)} = -\frac{2}{\pi} \cos(\varphi_1 - \varphi_2) \mathrm{P} \int_0^\infty d\omega \frac{\omega^2 \beta'(\omega)}{\omega^2 - \omega_0^2} \times e_l^{(\omega,+,+)}(r_1) e_l^{(\omega,+,+)*}(r_2) \cos \beta(z_1 - z_2),$$

$$W_{r\varphi}^{(g)} = -\frac{2i}{\pi} \sin(\varphi_1 - \varphi_2) \mathrm{P} \int_0^\infty d\omega \frac{\omega^2 \beta'(\omega)}{\omega^2 - \omega_0^2} \times e_r^{(\omega,+,+)}(r_1) e_\varphi^{(\omega,+,+)*}(r_2) \cos \beta(z_1 - z_2),$$

$$W_{zr}^{(g)} = -\frac{2i}{\pi} \cos(\varphi_1 - \varphi_2) \mathrm{P} \int_0^\infty d\omega \frac{\omega^2 \beta'(\omega)}{\omega^2 - \omega_0^2} \times e_z^{(\omega,+,+)}(r_1) e_r^{(\omega,+,+)*}(r_2) \sin \beta(z_1 - z_2),$$

$$W_{z\varphi}^{(g)} = \frac{2}{\pi} \sin(\varphi_1 - \varphi_2) \mathrm{P} \int_0^\infty d\omega \frac{\omega^2 \beta'(\omega)}{\omega^2 - \omega_0^2} \times e_z^{(\omega,+,+)}(r_1) e_\varphi^{(\omega,+,+)*}(r_2) \sin \beta(z_1 - z_2), \tag{C2}$$

and

$$W_{ll}^{(r)} = -\frac{2}{\pi} \mathrm{P} \int_0^\infty d\omega \frac{\omega^2}{\omega^2 - \omega_0^2} \sum_m \int_0^{kn_2} d\beta \cos m(\varphi_1 - \varphi_2) \times e_l^{(\omega,\beta,m,+)}(r_1) e_l^{(\omega,\beta,m,+)*}(r_2) \cos \beta(z_1 - z_2),$$

$$W_{r\varphi}^{(r)} = -\frac{2i}{\pi} \mathrm{P} \int_0^\infty d\omega \frac{\omega^2}{\omega^2 - \omega_0^2} \sum_m \int_0^{kn_2} d\beta \sin m(\varphi_1 - \varphi_2) \times e_r^{(\omega,\beta,m,+)}(r_1) e_\varphi^{(\omega,\beta,m,+)*}(r_2) \cos \beta(z_1 - z_2),$$

$$W_{zr}^{(r)} = -\frac{2i}{\pi} \mathrm{P} \int_0^\infty d\omega \frac{\omega^2}{\omega^2 - \omega_0^2} \sum_m \int_0^{kn_2} d\beta \cos m(\varphi_1 - \varphi_2) \times e_z^{(\omega,\beta,m,+)}(r_1) e_r^{(\omega,\beta,m,+)*}(r_2) \sin \beta(z_1 - z_2),$$

$$W_{z\varphi}^{(r)} = \frac{2}{\pi} \mathrm{P} \int_0^\infty d\omega \frac{\omega^2}{\omega^2 - \omega_0^2} \sum_m \int_0^{kn_2} d\beta \sin m(\varphi_1 - \varphi_2) \times e_z^{(\omega,\beta,m,+)}(r_1) e_\varphi^{(\omega,\beta,m,+)*}(r_2) \sin \beta(z_1 - z_2). \tag{C3}$$

Due to the relations (A9) and (B9), all the coefficients $W_{l_1 l_2}^{(g)}$ and $W_{l_1 l_2}^{(r)}$ are real parameters, and so are the cross-frequency shifts $\Omega_{12}^{(g)}$ and $\Omega_{12}^{(r)}$. Note that Eqs. (C2) and (C3) contain integrals over β. Therefore, $W_{l_1 l_2}^{(g)}$ and $W_{l_1 l_2}^{(r)}$ decrease to zero with increasing $|z_2 - z_1|$. Consequently, in the limit of large $|z_2 - z_1|$, all the cross-frequency-shift coefficients $\Omega_{12}^{(g)}$, $\Omega_{12}^{(r)}$, and Ω_{12} can be neglected, as in the case of two atoms in free space.

[1] J. I. Gersten and A. Nitzan, Chem. Phys. Lett. **104**, 31 (1984).
[2] L. M. Folan, S. Arnold, and S. D. Druger, Chem. Phys. Lett. **118**, 322 (1985).
[3] S. Arnold, S. Holler, and S. D. Druger, *Optical Processes in Microcavities* (World Scientific, Singapore, 1996), pp. 285–313.
[4] G. S. Agarwal and S. Dutta Gupta, Phys. Rev. A **57**, 667 (1998).
[5] M. Hopmeier, W. Guss, M. Deussen, E. O. Göbel, and R. F. Mahrt, Phys. Rev. Lett. **82**, 4118 (1999).
[6] W. L. Barnes and P. Andrews, Nature (London) **400**, 505 (1999); P. Andrews and W. L. Barnes, Science **290**, 785 (2000).
[7] R. L. Hartman and P. T. Leung, Phys. Rev. B **64**, 193308 (2001).
[8] D. M. Basko, J. Lumin. **110**, 359 (2004); D. M. Basko, F. Bassani, G. C. La Rocca, and V. M. Agranovich, Phys. Rev. B **62**, 15962 (2000).
[9] Ho Trung Dung, L. Knöll, and D.-G. Welsch, Phys. Rev. A **66**, 063810 (2002).
[10] S. A. Crooker, J. A. Hollingsworth, S. Tretiak, and V. I. Klimov, Phys. Rev. Lett. **89**, 186802 (2002).
[11] P. Andrew and W. L. Barnes, Science **306**, 1002 (2004).
[12] C. Hettich, C. Schmitt, J. Zitzmann, S. Kühn, I. Gerhardt, and V. Sandoghdar, Science **298**, 385 (2002).
[13] *Near-Field Optics*, edited by D. W. Pohl and D. Courjon, NATO Advanced Study Institute, Series B: Physics (Kluwer, Dordrecht, 1993).
[14] *Nano-Optics*, edited by S. Kawata, M. Ohtsu, and M. Irie (Springer, Berlin, 2002).
[15] Ho Trung Dung, S. Scheel, D.-G. Welsch, and L. Knöll, J. Opt. B: Quantum Semiclassical Opt. **4**, 5169 (2002).
[16] V. V. Klimov and V. S. Letokhov, Phys. Rev. A **58**, 3235 (1998).
[17] Fam Le Kien, S. Dutta Gupta, V. I. Balykin, and K. Hakuta, Phys. Rev. A **72**, 032509 (2005).
[18] T. Søndergaard and B. Tromborg, Phys. Rev. A **64**, 033812 (2001).
[19] H. Nha and W. Jhe, Phys. Rev. A **56**, 2213 (1997).
[20] V. V. Klimov and M. Ducloy, Phys. Rev. A **69**, 013812 (2004).
[21] V. I. Balykin, K. Hakuta, F. L. Kien, J. Q. Liang, and M. Morinaga, Phys. Rev. A **70**, 011401(R) (2004); Fam Le Kien, V. I. Balykin, and K. Hakuta, *ibid.* **70**, 063403 (2004).
[22] R. H. Dicke, Phys. Rev. **93**, 99 (1954).
[23] M. Gross and S. Haroche, Phys. Rep. **93**, 301 (1982).
[24] C. M. Caves and D. D. Crouch, J. Opt. Soc. Am. B **4**, 1535

(1987); K. J. Blow, R. Loudon, S. J. D. Phoenix, and T. J. Shepherd, Phys. Rev. A **42**, 4102 (1990); P. Domokos, P. Horak, and H. Ritsch, *ibid.* **65**, 033832 (2002).

[25] See, for example, D. Marcuse, *Light Transmission Optics* (Krieger, Malabar, FL, 1989); A. W. Snyder and J. D. Love, *Optical Waveguide Theory* (Chapman and Hall, New York, 1983).

[26] A. Takada and K. Ujihara, Opt. Commun. **160**, 146 (1999).

[27] See, for example, N. Vats, S. John, and K. Busch, Phys. Rev. A **65**, 043808 (2002).

[28] R. J. Cook and P. W. Milonni, Phys. Rev. A **35**, 5081 (1987); X.-P. Feng and K. Ujihara, *ibid.* **41**, 2668 (1990); Ho Trung Dung and K. Ujihara, *ibid.* **60**, 4067 (1999); Fam Le Kien, Nguyen Hong Quang, and K. Hakuta, Opt. Commun. **178**, 151 (2000).

[29] E. Arimondo, Prog. Opt. **35**, 257 (1996).

[30] M. O. Scully and M. S. Zubairy, *Quantum Optics* (Cambridge University Press, Cambridge, U.K., 1997), Chap. 7.

[31] G. S. Agarwal, *Quantum Optics*, Springer Tracts in Modern Physics Vol. 70 (Springer-Verlag, Berlin, 1974).